Genotype-Specific Spatial Distribution of Starch Molecules in the Starch Granule: A Combined CLSM and SEM Approach

Mikkel A. Glaring,[†] Christian B. Koch,[‡] and Andreas Blennow*[,†]

Plant Biochemistry Laboratory, Center for Molecular Plant Physiology (PlaCe), Department of Plant Biology and Department of Natural Sciences, The Royal Veterinary and Agricultural University, 40 Thorvaldsensvej, DK-1871 Frederiksberg C, Copenhagen, Denmark

Received March 8, 2006; Revised Manuscript Received May 19, 2006

Starch granule types from a variety of botanical sources were selected to represent differences in crystalline polymorph, amylose and phosphate content, and amylopectin chain length distribution. Equimolar labeling of starch molecules with the fluorophore 8-amino-1,3,6-pyrenetrisulfonic acid (APTS) was used to construct a detailed map of the distribution of amylose and amylopectin within the granule by confocal laser scanning microscopy (CLSM) analysis. Medium- and high-resolution scanning electron microscopy (SEM) were used to provide detailed images of granule surface structures. By using a combined surface and internal imaging approach, interpretations of a number of previous structural observations is presented. In particular, internal images of high amylose maize and potato suggest that multiple initiations of new granules are responsible for the compound or elongated structures observed in these starches. CLSM optical sections of rice granules revealed an apparent altered distribution of amylose in relation to the proposed growth ring structure, hinting at a novel mechanism of starch molecule deposition. Well-described granule features, such as equatorial grooves, channels, cracks, and growth rings were documented and related to both the internal and external observations. A new method for probing the phosphate distribution in native granules was developed using a phosphate-binding fluorescent dye and CLSM.

Introduction

Starch represents the major storage product of most plants. In contrast to the transient starch found in photosynthetic tissues, storage starch accumulates in the plastids of starch storing tissues such as tubers and seeds over long periods of time to form large, well-organized granular structures. Starch granules are made up of two structurally distinct polymers of glucose. Amylose constitutes about 20−40% of typical storage starch and consists of mainly linear chains of glucose linked by α-1,4-glucosidic bonds. Amylopectin constitutes the remaining 60−80% of the granule and is a much larger, highly branched polymer in which linear chains of α-1,4-linked glucoses are joined together by α-1,6-glucosidic bonds. These α-1,6-linked branch points are not randomly distributed but are clustered into an ordered arrangement allowing adjacent linear segments to form double helices. It is now widely accepted that the double helices formed by interacting chains of amylopectin form the basis for the crystalline structure of starch and are ordered into concentric crystalline lamellae interrupted by amorphous lamellae containing the branch points.[1] The semicrystalline stacks consisting of the alternating lamellae form concentric rings embedded in a layered background of amorphous material. These alternating 120−400 nm regions give rise to the growth rings that are visible under a light microscope in some granules. Other levels of granule structure have been suggested as intermediates between the lamellae structure and the growth rings. Oostergetel and van Bruggen[2] suggested a structure in which the amylopectin is arranged into interconnected superhelices with a central 8 nm cavity. Gallant and co-workers[3] provided evidence that lamellae are organized into spherical structures termed blocklets. These blocklets range in diameter from 20 to 500 nm depending on the starch type and the location in the granule.

Native starch granules can be characterized by two X-ray diffraction patterns depending on the packing of amylopectin double helices.[4] The A-type is characteristic of the cereal starches and the B-type of tuber and high amylose starches. A C-type, which is a mixture of A- and B-type diffraction patterns, has also been identified and is characteristic of many legume starches. The V-form is a term for single helices of amylose cocrystallized with other compounds such as iodine or lipids. By studying the relationship between the distribution of amylopectin chain lengths and starch crystalline structure, it was suggested that chain lengths are a major determinant of crystalline polymorph. In general, amylopectin from A-type starches have shorter average chain lengths and a larger proportion of shorter chains than amylopectin from B-type starches.[5]

It has been demonstrated that the synthesis of amylose occurs inside the granule,[6] though the distribution of amylose within the amylopectin matrix has not been unequivocally determined. The absence of amylose has no influence on the formation of the granule matrix or the degree of crystallinity,[7,8] and starches with little or no amylose still contain visible growth rings. In native starch granules, amylose appears to be interspersed among the amylopectin molecules,[9] and it has generally been assumed that amylose resides primarily in the amorphous regions of the granule. In support of this, blue-staining growth rings in potato granules have been observed by iodine staining.[10,11] Moreover, visualization of growth ring structures in potato granules by APTS (8-amino-1,3,6-pyrenetrisulfonic acid) staining is strictly dependent on amylose concentration.[12] Earlier reports have suggested that amylose is more concentrated near the granule surface.[13] More recent data from enzyme−gold labeling experi-

* To whom correspondence should be addressed. Phone: + 45 35283334. Fax: +45 35283333. E-mail: abl@kvl.dk.
[†] Plant Biochemistry Laboratory.
[‡] Department of Natural Sciences.

10.1021/bm060216e CCC: $33.50
Published on Web 06/27/2006

ments and iodine staining of hydrated maize and potato granules indicate that amylose is localized in distinct amorphous regions around the hilum.[11] This finding has been supported by APTS staining of potato starch granules.[12]

In addition to amylopectin and amylose, a number of minor components influence the physical and chemical properties of starch. The only known naturally occurring covalent modification of starch is phosphorylation. The phosphate monoesters are incorporated into starch during biosynthesis[14] and have profound effects on both the physical properties of starch and its degradation in the plant.[15] The level of phosphorylation varies greatly with the botanical source, with tuberous starches containing high amounts of phosphate (0.2−0.4% phosphorylated glucose units in potato) and cereal storage starches containing little or no starch-bound phosphate. Phosphate groups are bound as monoesters at the C-6 or C-3 position of the glucosyl units of amylopectin.[15] Other sources of phosphate in starch granules include internal phospholipids and inorganic phosphate.[16] In root and tuber starches, phosphate is primarily found as monoesters, whereas phosphate in cereals is predominately in the form of phospholipids.[17] An exception to this is the *waxy* (high amylopectin) cereal starches which contain only minute amounts of total phosphate.[17] Jane and Shen[13] reported that the concentration of phosphate monoesters was higher in the core of potato granules, and a recent particle-induced X-ray emission (PIXE) study on potato granules has confirmed these result.[18] It has been determined that a major part of the monoesterified phosphate groups are located in the amorphous regions.[19] The presence of internal lipids is a characteristic of cereal starches. In some cases, they constitute more than 1% of the dry weight.[1] The amount of lipid is positively correlated to amylose content, presumably as a consequence of their ability to form complexes with amylose.[20] Small amounts of protein can also be found inside the starch granule. Many of these proteins are directly involved in biosynthesis, such as granule-bound starch synthase[6] and some isoforms of starch branching enzyme and the soluble starch synthases;[21,22] other proteins may just have been trapped by the growing granule.

The internal structure of native starch granules can be considered a remnant of starch granule biosynthesis. In storage starches, these structures have been generated as a combined result of biosynthetic and degradative metabolic reactions and physical assembly processes of the growing macromolecules. Hence, imaging of these structures is indicative of the history of starch granule assembly and yields information about important events that have taken place during the growth of the granule. The structures that can be assessed include deposition patterns of starch molecules, phosphate esters, and other minor components, internal cavities, and cracking that took place where tension developed during granule growth, channels and holes formed in cereal granules, as well as granule initiation. By simultaneously monitoring the development of these structures, the general chronological order of these events may be elucidated.

Over the past few decades, granule structure and topography have been extensively studied using a variety of microscopy techniques. Scanning electron microscopy (SEM) has permitted detailed morphological characterization of starch granules,[23] and both SEM and transmission electron microscopy (TEM) have been used to visualize the proposed blocklet structure of starch.[3] Confocal laser scanning microscopy (CLSM) has been successfully used to study a number of different granule features, including cavities and growth rings,[24] channels,[25] protein content,[26] and the process of gelatinization.[24] Recently, a method for visualizing the distribution of amylose and amylopectin in starch granules was developed using the fluorophore APTS.[12] APTS reacts specifically with the reducing ends of starch molecules leading to a 1:1 stoichiometric ratio of starch molecule labeling. Because of its smaller size, amylose contains a much higher molar ratio of reducing ends per glucose residue than amylopectin. This results in a higher by-weight labeling of amylose enabling the distinction of the two molecules by confocal laser scanning microscopy (CLSM). The intense and stable fluorescence of APTS allows both surface and internal images of starch granules to be recorded at high resolution. Access to the interior of the granule for the larger fluorescent dyes could be influenced by the overall porosity of the granule. APTS (molecular weight (M_w) of 523 g/mol) penetrates potato starch granules[12] as does merbromin (M_w 751 g/mol).[26,27] Both of these compounds are negatively charged. Other fluorescent compounds that have been successfully used include rhodamine B (M_w 479 g/mol) and safranin O (M_w 365 g/mol).[24] A study on starch granule porosity determined that carbohydrates with a molecular mass of more than 1000 g/mol are excluded from the granule as are molecules with a hydrodynamic radius above 0.6 nm.[28] Thus, while the starch granule can be considered to be a porous structure, some larger fluorescent dyes might be excluded from the granule matrix. A notable exception to this porosity exclusion is the presence of channels in many cereal starches, which allow access to the granule interior for much larger molecules such as proteins.

In this study, CLSM imaging, using APTS as a probe for starch molecule distribution and Pro-Q Diamond as a specific probe for phosphate, was used in conjunction with SEM to study the relationship between internal and external structural features of starches extracted from different botanical sources and genetic backgrounds. The investigation has focused on characterizing the genotype-specific internal deposition of starch molecules and how this is manifested at the surface of the granule. Molecular properties such as amylose and phosphate content and amylopectin chain length distribution were related to the structural data revealing the influence of these features on starch granule structure. Specific internal phenomena of starch granule biogenesis were revealed, including growth ring propagation near the granule surface and aberrant initiation leading to compound granule structures.

Experimental Section

Starch Sources. Maize starches were provided by Cerestar-AKV I/S (Denmark). The wheat starch was provided by Semper AB (Sweden). Barley starch was obtained from Svalöf-Weibull AB (Sweden). The tapioca, pea, and rice starches were obtained from KMC (Brande, Denmark). Potato starch with suppressed levels of GBSS (high amylopectin) was obtained from Lyckeby Stärkelsen (Sweden). Potato starch from plants with reduced levels of starch branching enzymes I and II (high amylose) was obtained from Danisco Biotechnology (Copenhagen, Denmark). Starch from a potato line with antisense suppressed GWD protein (low phosphate),[29] normal potato, and rhizomes of *Curcuma zedoaria* was prepared as described elsewhere.[12,30]

Starch Compositional Analysis. The amylopectin chain length distribution was determined following enzymatic hydrolysis of the α-1,6-branch linkages using isoamylase. Generated linear oligosaccharides were separated using high-performance anion-exchange chromatography (HPAEC) with pulsed amperometric detection (PAD) on a Dionex DX500 system as previously described.[31] For analysis of starch-bound phosphate, 20 mg of starch was hydrolyzed to its monomeric constituents for 4 h in 1 mL of 0.7 M HCl at 100 °C. Samples were neutralized with 2 M NaOH and subjected to HPAEC analysis as

Table 1. Starch Sources and Characteristics[a]

starch source	amylose % (±SE)	phosphate[b] (±SE)	mean DP (±SE)	polymorph[c]
maize (*Zea mays*)				
normal	45.3 (±0.78)	0.11 (±0.0)	24.1 (±0.1)	A
high amylose	60.3 (±1.51)	1.32 (±0.1)	29.5 (±0.3)	B + V[d]
waxy	not detected	0.09 (±0.0)	24.7 (±0.2)	A
potato (*Solanum tuberosum*)				
normal	27.6 (±0.11)	23.2 (±0.6)	27.2 (±0.3)	B
low phosphate	38.5 (±0.45)	1.40 (±0.1)	26.7 (±0.1)	B
high amylose	41.0 (±0.94)	60.0 (±1.3)	29.5 (±0.7)	B
high amylopectin	2.10 (±0.50)	18.1 (±0.4)	26.7 (±0.0)	B
tapioca (*Manihot esculenta*)	31.6 (±0.28)	1.11 (±0.1)	26.4 (±0.4)	C
pea (*Pisum sativum*)	55.0 (±0.17)	0.48 (±0.1)	25.6 (±0.4)	C[e]
wheat (*Triticum aestivum*)	45.3 (±0.33)	0.20 (±0.1)	24.0 (±0.2)	A
barley (*Hordeum vulgare*)	52.6 (±0.60)	0.12 (±0.0)	24.4 (±0.0)	A
rice (*Oryza sativa*)				
normal	32.8 (±0.95)	0.45 (±0.2)	23.5 (±0.4)	A
high amylopectin	not detected	0.28 (±0.0)	24.6 (±0.3)	A
Curcuma zedoaria	41.8	58.8	28.5 (±0.0)	B

[a] Values for amylose and phosphate content and mean degree of polymerization (mean DP) were obtained as described in the Experimental Section. Amylose and phosphate values for *Curcuma zedoaria* were obtained elsewhere.[12] Values in paranthesis represent standard error (±SE). [b] Concentration of phosphate monoesters in nanomole of glucose-6-phosphate per milligram starch. [c] Data on the crystalline polymorph were obtained from recent reviews of the literature[19,34] except where indicated. [d] Ref 35. [e] Ref 8.

previously described[32] using glucose-6-phosphate as a standard (Sigma-Aldrich, catalog no. G-6526). The amylose content of starch was determined by colorimetric staining[33] using an iodine solution (0.26 g I_2 and 2.6 g KI in 10 mL water, diluted 1000 times in 100 mM HCl before use). 10 mg of starch was dissolved in 5 mL of 1 M NaOH with vigorous stirring overnight. 10 μL of this sample was added to 200 μL of the diluted iodine solution in an Elisa plate, and absorbance was measured at 550 and 620 nm after 2−3 min. Amylose levels were calculated by plotting the A_{620}/A_{550} ratio against a standard curve of amylose. Potato amylose (type III, Sigma-Aldrich, catalog no. A-0512) and potato amylopectin (Sigma-Aldrich, catalog no. A-8515) were treated as the starch samples and subsequently mixed to form standard solutions of 0−60% amylose in amylopectin.

APTS Staining. APTS staining was performed essentially as previously described.[12] Starch granules (2−4 mg) were incubated in 4 μL APTS solution (20 mM 8-amino-1,3,6-pyrenetrisulfonic acid (Molecular Probes) dissolved in 15% acetic acid) and an equal volume of 1 M sodium cyanoborohydride. The mixture was incubated at 30 °C for 15−18 h. The granules were then washed five times in distilled water and suspended in 20 μL of 50% glycerol. For microscopy, 1 μL of the granule preparation was fixed in a mixture containing 2% agar and 80% glycerol in water on a glass slide.

Pro-Q Diamond Staining. Starch granules of normal potato and *Curcuma zedoaria* were ground in liquid nitrogen to expose internal surfaces prior to staining. Protease treatment was carried out by incubating in a protease mixture (50 mM Tris-HCl pH 7.5, 10 mM $CaCl_2$, 1 mg/mL of both Trypsin and Proteinase K) for 4 h at 37 °C. Samples were then washed twice in an SDS buffer (0.1% SDS, 5 mM EDTA, 50 mM Tris-HCl pH 8.0) and three times in distilled water. For Pro-Q staining, granules were mixed with 500 μL Pro-Q Diamond phosphoprotein gel stain (Molecular Probes) and incubated for 1 h at room temperature followed by 3 washes in distilled water. Granules were suspended in 50% glycerol, and 1 μL was mixed with 5 μL od 80% glycerol on a glass slide. SYPRO Ruby (Molecular Probes) staining was accomplished by a similar approach.

Confocal Laser Scanning Microscopy (CLSM). Images of APTS and Pro-Q stained granules were recorded on a confocal laser scanning microscope (TCS SP2, Leica Microsystems, Germany) as previously described.[12] For APTS, a 488 nm laser line was used for excitation, and light was detected between 500 and 535 nm. A laser power of 25% was maintained during acquisition of all APTS images, and the gain was varied to prevent saturation of the detector and to ensure comparable fluorescence intensities in all images. For Pro-Q, a 543 nm laser line was used for excitation, and light was detected in the interval from 570 to 600 nm. For quantification purposes, the laser power was kept constant at 50%, and images were recorded at maximum gain for all samples. The objectives used were 40× plan apo/1.25−0.75 Oil and 63× plan apo/1.32−0.6 Oil CS. 3D image analysis was performed with the TCS SP2 software.

Scanning Electron Microscopy (SEM). Starch granules were separated by gentle grinding and prepared for observation of external and internal features by Pt coating for up to 16 min at 900 V. The coated granules were observed using a Philips XL20 working at a high tension of 2 kV and a working distance down to approximately 2.5−3 mm.

Results

Starch Compositional Analysis. In the present work, starch granules were prepared from a wide selection of starch crop genotypes representing starches with different amylose and phosphate content, amylopectin chain length distribution, and crystalline polymorph (Table 1). The cereal starches represent A-type crystalline polymorphs with very low levels of phosphate and shorter average chain lengths. The potato starches represent the B-type polymorph and display a wide range of phosphate content and longer average chain lengths. Tapioca and pea starch, both C-type crystalline polymorphs, were chosen as intermediate starches with slightly higher phosphate levels than the cereals and an average chain length value between the tuberous and cereal starches. High amylose starches were selected from maize and potato. These starches show increased chain lengths compared to their normal and high amylopectin counterparts and are both B-type polymorphs. The low amylose (high amylopectin) starches represent both A-type (maize and rice) and B-type (potato) crystalline polymorphs. They have slightly lower phosphate content but average chain lengths comparable to their normal counterparts. Starch extracted from the rhizomes of the ginger *Curcuma zedoaria* was selected for its high phosphate content. A potato line engineered for reduced levels of the starch phosphorylating enzyme GWD (α-glucan, water dikinase) was used as a source of low-phosphate potato starch.[29]

APTS Staining, CLSM and SEM. The selected starches were stained with the fluorophore APTS and analyzed by

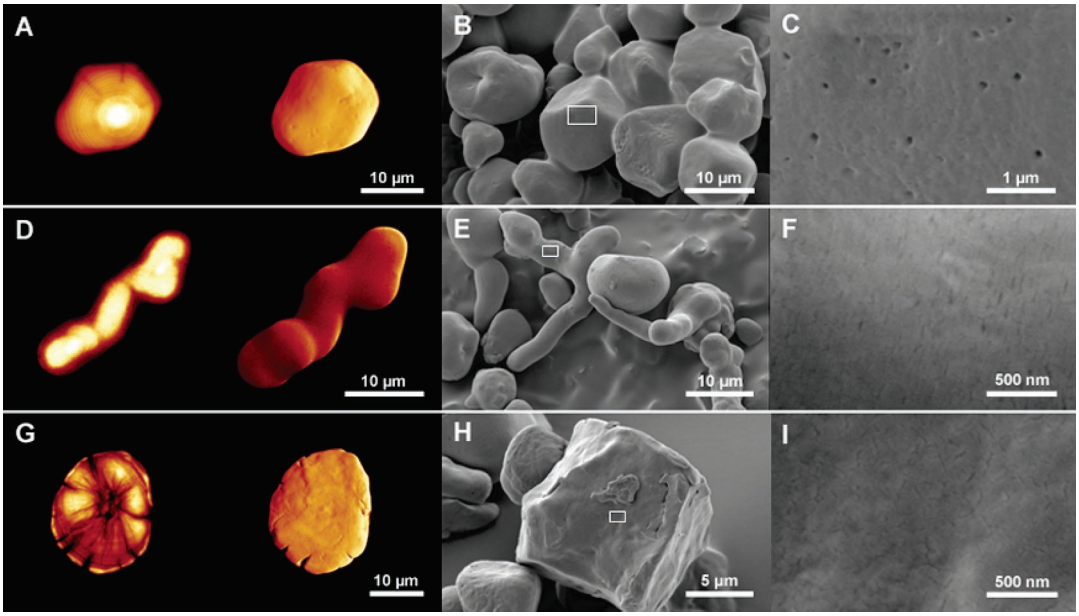

Figure 1. Maize starch granules. Normal (A−C), high amylose (D−F), and *waxy* maize (G−I). CLSM optical cross section and surface image (A,D,G). Micrometer (B,E,H) and nanometer (C,F,I) scale SEM images. The white squares indicate the areas viewed in the nanometer scale images. Scale bars as indicated.

CLSM. Specific internal structures, such as growth rings, channels, and cracks, as well as the general molecular distribution of amylose and amylopectin within the granule, were investigated. External features, such as size and shape, were then related to the internal observations. SEM was used to complement the CLSM images in an effort to reveal details about the granule surface which could not be distinguished by CLSM. SEM images were recorded at several levels of magnification enabling characterization of both micrometer and nanometer structural features. This approach has for the first time allowed a detailed investigation and interpretation of internal and topographical features of starches from a wide selection of starch crop genotypes. This has led to a number of new observations, including internal imprints of the equatorial grooves in cereals, a potential influence of amylose on starch granule initiation and formation of compound structures, as well as evidence of specific mechanisms that determine directional growth and granule shape.

Maize Starch Types. Granules from normal maize were mostly regular and polyhedric (Figure 1B). CLSM optical sections showed an intensely stained centered or slightly eccentric hilum and regular round growth rings (Figure 1A). The growth rings were often cut off at the surface, suggesting that the shape of the granule is determined by physical interaction with neighboring granules and not by the deposition of growth rings. Channels were visible as dark lines running from the surface toward the hilum, penetrating the growth rings without any disturbances at the border (Figure 1A). Starch granules that were not protease-treated (see Materials and Methods) showed fluorescence in these channels suggesting the presence of proteins. A CLSM surface image showed small indentations at the surface of the granule, possibly representing channels exposed to the surface (Figure 1A). High-magnification SEM images showed frequent 50−100 nm holes at the surface, confirming the presence of putative channel openings (Figure 1C).

The high amylose maize starch had smoother and more rounded granules than normal maize. Some of the granules were elongated, filamentous structures with multiple growth directions (Figure 1E). These granules formed a distinct subpopulation among the more common rounded granules. CLSM optical sections of both the round and elongated granules revealed a brightly stained interior consistent with the high amylose content (Figure 1D). The APTS staining pattern of the elongated granules revealed multiple highly fluorescent round structures, which appeared to make up the interior of these granules. This observation is consistent with the presence of multiple hila arranged like a string of pearls inside the elongated structure (Figure 2A) and suggests that aberrant initiation of new granules could be the cause of this phenomenon. Alternatively, these structures could have been formed by the fusion of several smaller granules, though this seems unlikely given their smooth surface topography. Some of the rounded granules also appeared to contain multiple hila (Figure 2A, top left). Growth rings were generally difficult to see by APTS staining, presumably because of the substantial amounts of amylose, which appeared to be irregularly deposited in the granule matrix. Figure 2B shows a large irregular granule where growth rings are visible near the

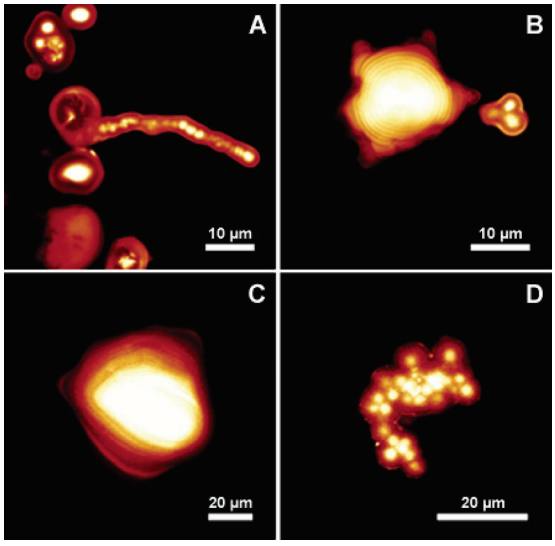

Figure 2. CLSM optical sections showing growth ring structure and multiple initiations in high amylose granules from maize (A and B) and potato (C and D). Scale bars as indicated.

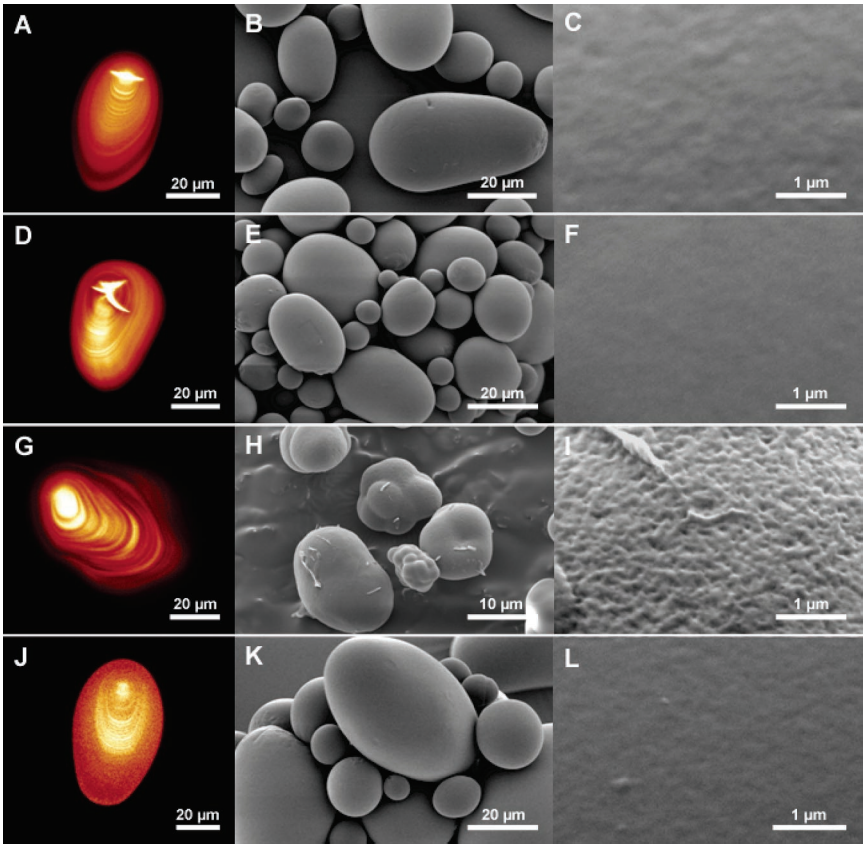

Figure 3. Potato starch granules. Normal (A−C), low phosphate (D−F), high amylose (G−I), and high amylopectin potato (J−L). CLSM optical cross sections (A,D,G,J). Micrometer (B,E,H,K) and nanometer (C,F,I,L) scale SEM images. Scale bars as indicated.

surface. As with normal maize, these growth rings are synthesized as round regular rings and do not appear to follow the shape of the outside surface. The irregular surface of this granule would suggest that the shape has been determined by other mechanisms than physical interaction with neighboring granules. Channels were not visible in CLSM optical sections as they were in normal maize, but SEM images confirmed the presence of putative channel openings at the surface (data not shown). Interestingly, these openings were only observed in the round granules and not in the elongated structures (Figure 1F).

Granules from *waxy* maize were more irregular and rough than normal maize granules (Figure 1H), though the polyhedric shape could still be recognized. As a consequence of the low amylose content, APTS staining was more uniform, with darker hila, and less intense than in the other maize starches. The hila were often labeled with a very small fluorescent dot (data not shown). A large proportion of the larger granules showed severe internal radial cracking substantiating the importance of moderate amylose concentration for maintaining the integrity of the starch granule (Figure 1G). A CLSM surface image showed that some of these cracks reached the surface, giving a rough appearance to the granule (Figure 1G). Internal cracking was also seen in some of the larger granules of both normal and high amylose maize, but this was much less frequent and could rarely be seen at the surface (data not shown). Growth rings were visible despite the lack of amylose and did not follow the surface shape. Channels could be seen by both CLSM and SEM but appeared to be less frequent or more difficult to discern than in normal maize starch. This was previously observed in a CLSM study of merbromin-stained maize granules.[25] Despite the rough appearance of the granules, they were as smooth as the other maize starches at the nanometer scale (Figure 1I).

Potato Starch Types. As revealed by SEM, the starch granules from normal potato tubers were smooth with a spherical or ellipsoid shape (Figure 3B). CLSM optical sections showed clear growth rings around an eccentric brightly stained hilum (Figure 3A). Granule surfaces were smooth with only minor ripples or bumps at the nanometer scale (Figure 3C). The shape and surface structure of granules from the low phosphate tubers (antisense GWD) were indistinguishable from normal potato granules (Figure 3E,F). Optical sections showed clear growth rings but a higher frequency of cracking near the hilum (Figure 3D). This observation was also made by Blennow et al.[12] who speculated that the observed fractures could be the effect of long-range destabilizations due to the decreased phosphate content or the increased amylose content.

Starch granules from the high amylose potato tubers (suppressed starch branching enzyme) were significantly different from the other potato granules. SEM images showed rough, lumpy shapes (Figure 3H), and CLSM optical sections revealed a large bright hilum surrounded by thick growth rings following the outside surface (Figures 3G and 2C). High-magnification images of the surface by SEM showed that it was more rough and irregular at the nanometer scale, clearly distinguishing these granules from the other examined potato granules (Figure 3I). Contrary to what was observed in both normal and high amylose maize, the deposition of growth rings appears to determine the external shape in these granules (compare Figures 2C and 2B). A number of granules had severe internal cracks which were often filled with a fluorescent substance (data not shown). Some structures appeared to be fusions of many smaller granules (Figure 3H). CLSM sections of these granules showed a multitude of small, round fluorescent structures resembling the "multiple-hila" structures seen in high amylose maize (compare

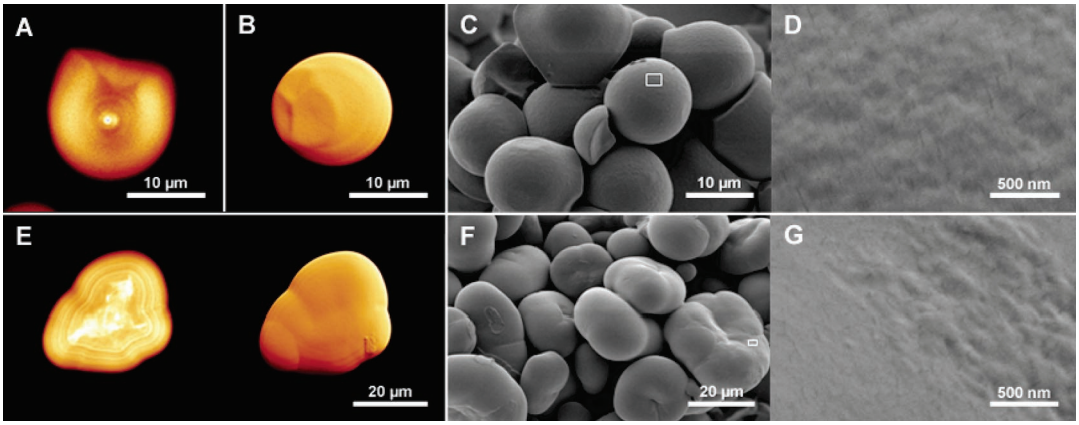

Figure 4. Tapioca (A−D) and pea (E−G) granules. CLSM optical cross sections (A,E) and surface images (B,E). Micrometer (C,F) and nanometer (D,G) scale SEM images. The white squares indicate the areas viewed in the nanometer scale images. Scale bars as indicated.

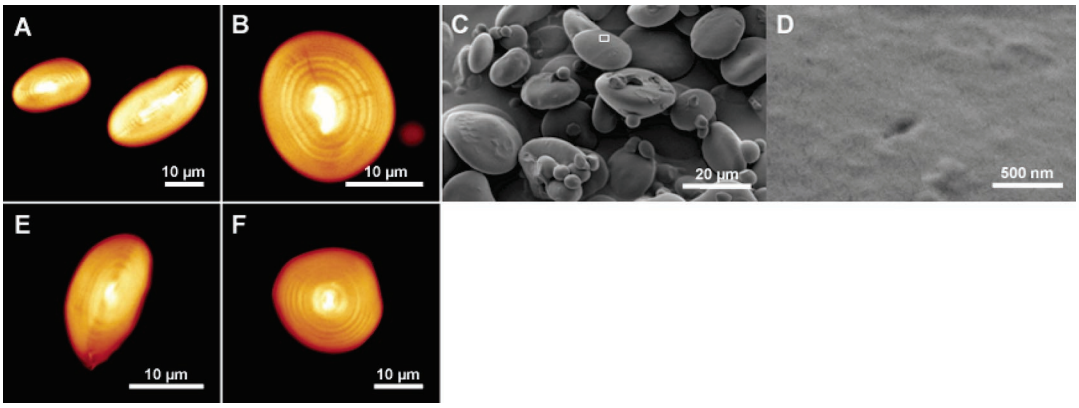

Figure 5. Wheat (A−D) and barley (E−F) granules. CLSM optical cross sections, side view (A,E), and top-down view (B,F). Micrometer (C) and nanometer (D) scale SEM images. The white square indicates the areas viewed in the nanometer scale image. Scale bars as indicated.

Figures 2D and 2A). The fact that these granules can be found as a distinct fraction in high amylose starches from both maize and potato points toward a possible influence of amylose on granule initiation in these starches. Evidence that the small round structures represent individually initiated granules was provided by polarized light microscopy. A characteristic maltese cross coinciding with the highly fluorescent center was observed in each of the small, rounded structures (data not shown). As with high amylose maize, these granules were too smooth to be simple conglomerates of smaller granules, and the fact that they were seen with both SEM and CLSM precludes the possibility that they represent artifacts of the SEM preparation.

Granules from the high amylopectin potato starch resembled the granules from normal and low phosphate starch in terms of size, shape, and surface structure (Figure 3K,L). CLSM images showed a weak uniform APTS staining of the granules consistent with the low amylose content (Figure 3J). For the sake of comparison, CLSM images of these granules were recorded at higher intensity leading to somewhat coarser images. Growth rings were weak or nonexistent and were only seen close to the hilum, suggesting that amylose is confined to the core of the granule. This is in agreement with previous results of iodine staining of low amylose potato granules.[10]

Tapioca and Pea Starch Types. Tapioca starch granules were smooth with irregular and truncated shapes. The shapes appeared to have been heavily influenced by physical interaction with other granules (Figure 4C). Optical sections showed a small fluorescent hilum surrounded by a darker area where regular round growth rings could be seen (Figure 4A). CLSM surface images clearly displayed the irregular shapes as cuts or depressions in the granules (Figure 4B). SEM images of the surface showed a slightly rippled structure (Figure 4D).

The pea granules were large, somewhat disc-shaped, multilobed structures (Figure 4F). The surfaces were generally smooth, though some rougher areas could be identified (Figure 4G). CLSM optical sections showed brightly stained granule features and clear growth rings (Figure 4E) with a hilum that was often irregular and difficult to identify by APTS staining, indicating a less defined starch granule initiation process. In contrast to the observation of growth rings in maize granules, the external shape of pea granules was clearly related to the deposition of growth rings. They were in all cases seen to follow the surface, suggesting that growth ring formation directs the bulbed shape of these granules (Figure 4E). An explanation for the irregularity of the growth rings could be the diffuse hilum identified in these granules, which might affect the synthesis of the initial growth rings. In contrast, the irregular shapes of the high amylose potato granules did not appear to be caused by an obvious disturbance of the hilum (see above and Figure 3G).

Wheat and Barley Starch Types. The wheat granule preparation contained both the disc-shaped A-type granules as well as the smaller, round B-type granules (Figure 5C). As imaged by SEM, the surfaces of the A-type granules were smooth with only minor ripples (Figure 5D). The A-type granules had a fluorescent hilum and clearly visible growth rings when viewed with CLSM. Channels going across the growth rings were seen in the larger A-type granules (Figure 5B). A side view of the disc-shaped granules revealed a flattened hilum and growth rings (Figure 5A). Furthermore, what appeared to

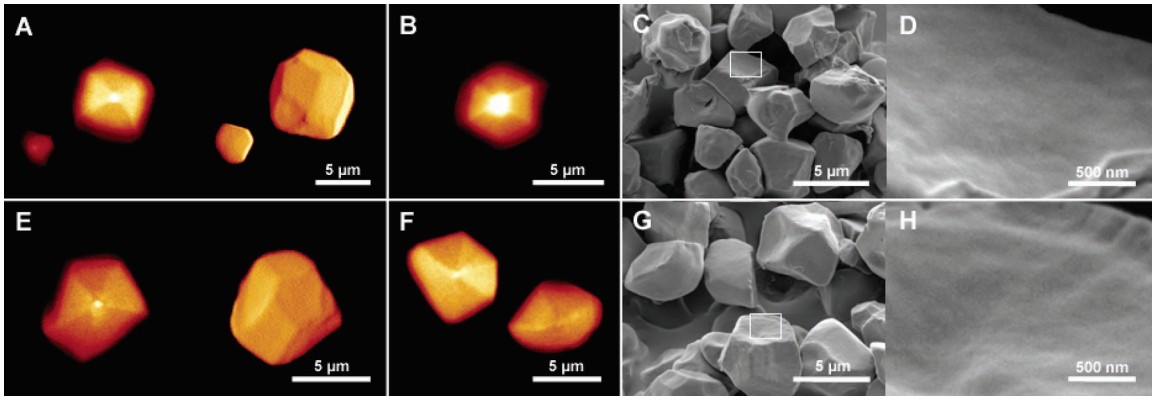

Figure 6. Normal (A−D) and high amylopectin (E−H) rice granules. CLSM optical cross sections (A,B,E,F) and surface images (A,E). Micrometer (C,G) and nanometer (D,H) scale SEM images. The white squares indicate the areas viewed in the nanometer scale images. Scale bars as indicated.

be an altered internal distribution of amylose was seen around the equatorial groove in many granules. This was visualized as a band of either brighter or darker fluorescence spanning the granule with growth rings going across (Figure 5A). Although the grooves appeared to have left an impression in the interior of the granule, we did not observe any of the characteristic equatorial grooves on the surface. The granules from barley showed shapes similar to wheat, with both large disc-shaped granules and smaller round granules. CLSM optical sections revealed that the internal structure was also similar to wheat except channels were not easily found, suggesting that they are less frequent (Figure 5F). Side views of disc-shaped granules showed the same altered distribution of amylose with a darker band running longitudinally across the granule (Figure 5E). As with wheat, no equatorial groove was seen on the outside of the granules (data not shown).

Rice Starch Types. Normal rice starch granules were irregularly shaped and polygonal (Figure 6C). The surface was generally smooth in high-magnification SEM images (Figure 6D). CLSM sections showed a brightly stained hilum and no visible growth rings (Figure 6A,B). A feature which appeared to be specific for rice starch was the presence of triangular shapes of more intense APTS staining, with one point anchored in the hilum and the opposite flat face situated at the edge of the granule (Figure 6A,B). The flat face of the triangles appeared to match the external edges of the granules, suggesting that the outside shape is determined by events taking place during the entire span of starch granule biogenesis. These data do not support the notion that the final shape of the granules is solely determined by restricted space in the closely packed endosperm. This is not unlike the effect of growth rings on the external structure of both pea and high amylose potato granules (see above), except that the deposition of amylose appears to be remarkably different in rice granules. SEM images showed that the high amylopectin rice granules were indistinguishable from normal rice granules, showing the same polygonal shape and smooth surface (Figure 6G,H). APTS staining was less intense, as expected for granules with insignificant amylose concentration. The hilum appeared as a small dot of fluorescence, and no growth rings were observed (Figure 6E,F). Despite the absence of amylose, the internal triangular shapes which extended from the hilum to the surface of normal rice granules were still visible. They were observed to align with the edges of the polygonal granules (Figure 6E,F), again suggesting that specific depositions of starch molecules determine the external shape of the granule.

Pro-Q Diamond as a Probe for Phosphate in Native Starch Granules. The Pro-Q Diamond dye is a metallo-organic fluorophore originally developed as a sensitive stain for phosphoproteins. It binds directly to the phosphate group irrespective of the underlying protein structure, allowing it to recognize a broad spectrum of phosphorylated proteins (Pro-Q Diamond phosphoprotein blot stain kit (P-33356), product information, Molecular Probes). We reasoned that Pro-Q might be able to recognize accessible phosphate groups in native starch granules. The distribution of Pro-Q fluorescence could then be taken as an indication of the phosphate distribution pattern in the granule. The specific properties of Pro-Q Diamond, including molecular weight and formula, are so far unavailable, but the results presented here suggest that the dye is capable of penetrating most starches under the conditions used. A molecular model of double-helical amylopectin suggests that phosphorylation at the C-6 position of the glucose residues is possible without disturbing double-helical integrity and the packing of double helices.[36] This would indicate a certain degree of steric hindrance for any compounds intended to interact with phosphate groups in the crystalline regions of the granule and suggests that not all phosphate groups are equally accessible.

Starch granules from cereal and tuberous sources representing a wide range of starch-bound phosphate contents were stained with Pro-Q. A preliminary screen under a standard fluorescence microscope showed clear binding of the dye to potato granules, and a subsequent CLSM analysis confirmed that fluorescence intensity was positively correlated to phosphate content (Figure 7). Furthermore, incubating granules in Pro-Q in the presence of glucose-6-phosphate, but not glucose, greatly diminished the binding of the dye to the granules, indicating a competitive interaction with phosphorylated glucose units (data not shown). Starch granules from normal and high amylose potato were stained brightly by Pro-Q, primarily near the surface (Figures 7C,D and 8B−D). As expected, the low-phosphate potato starch showed very little fluorescence (Figure 7E). Granules from normal potato were ground in liquid nitrogen to expose internal surfaces prior to staining. The fluorescence intensity was generally higher at the original granule surfaces than at the broken edges (data not shown), demonstrating that surface staining in potato is a consequence of specific structures that are not present in the interior of the granule, and is not simply due to unspecific interactions with the granule surface. The high amylose potato starch, generated by antisense inhibition of starch-branching enzymes, showed frequent cracks in the granule interior. The cavities formed by cracking did not stain with Pro-Q, even though the cracks were often close to the surface. Interestingly, the fluorescence in these granules appeared to be concentrated a few micrometers beneath the surface, indicating an altered distribution of phosphate compared to normal potato

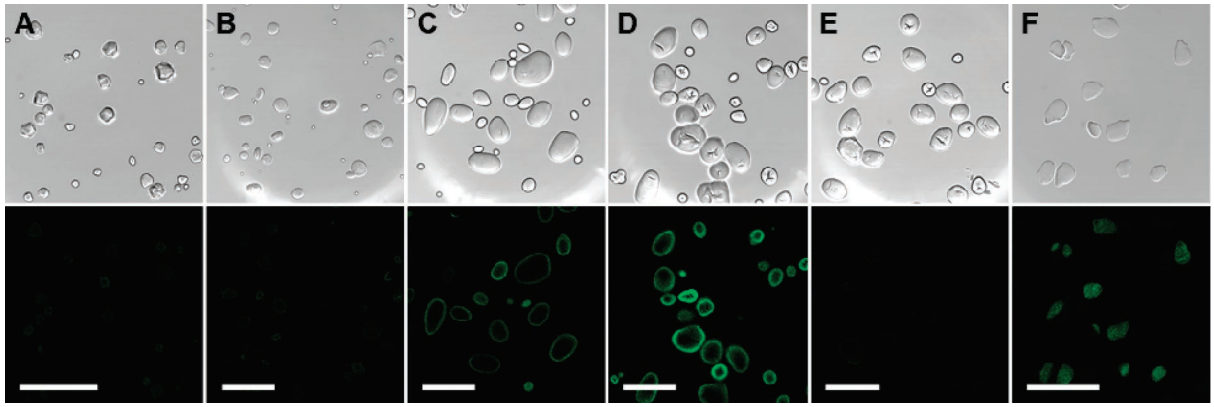

Figure 7. Pro-Q staining of starch granules. Transmission image (upper panel) and Pro-Q fluorescence (lower panel) of normal rice (A), wheat (B), normal potato (C), high amylose potato (D), low-phosphate potato (E), and *Curcuma zedoaria* (F). All images were recorded at the same laser power and instrument gain. Scale bar 100 μm.

starch (Figure 8D). It is worth noting that a transmission image is comparable to a standard light microscopy image, whereas the fluorescence image only represents a single focal plane. The highly phosphorylated starch granules from the ginger *Curcuma zedoaria* were uniformly stained at high intensity, sometimes with a slightly darker region around the hilum (Figure 7F). The cereal starches showed little fluorescence (Figure 7A,B). Both maize and wheat granules were uniformly stained (Figure 8A), though there was a tendency for increased surface staining in some granules of wheat. *Waxy* maize granules were only minimally stained, indicating that the fluorescent signal observed in normal maize (and possibly wheat) is at least partially an effect of Pro-Q binding to phospholipids (data not shown).

Staining with APTS had revealed channels in granules of both maize and wheat. These structures appeared as either dark or light channels in images of maize granules but were always dark in wheat granules (see above). Staining with Pro-Q showed fluorescence in channels of maize but not wheat (data not shown). This suggested that the bright APTS and Pro-Q fluorescence associated with some channels in maize could be caused by proteinaceous material. The presence of proteins in channels of maize has previously been observed by CLSM using a protein-specific dye.[26] This earlier observation was confirmed by staining with SYPRO Ruby, a general protein stain which showed clear channel fluorescence, and by protease treatment of starch granules which resulted in complete removal of fluorescence after Pro-Q staining (data not shown). The observation that Pro-Q binds to proteins in channels of maize would suggest that some of these proteins are phosphorylated, though it is not clear whether these proteins are native or are sequestered during the starch isolation procedure.

Discussion

CLSM has previously been used to characterize internal features of starch granules such as channels,[25] protein content,[26] and cavities and growth rings.[24] By using APTS staining, this basic structural information can be directly coupled to information about the amylose and amylopectin distribution in the granule. The conventional method of amylose staining with iodine is not compatible with CLSM, and though iodine staining has been successfully used to characterize amylose distribution,[10,11] CLSM on APTS stained granules has several advantages over conventional iodine staining. First, the ability to capture images from thin optical sections gives detailed information on the internal structure of the granule. Second, recording of image stacks allows three-dimensional reconstructions of granule surfaces, a feature usually associated with scanning electron microscopes. The stability and high intensity

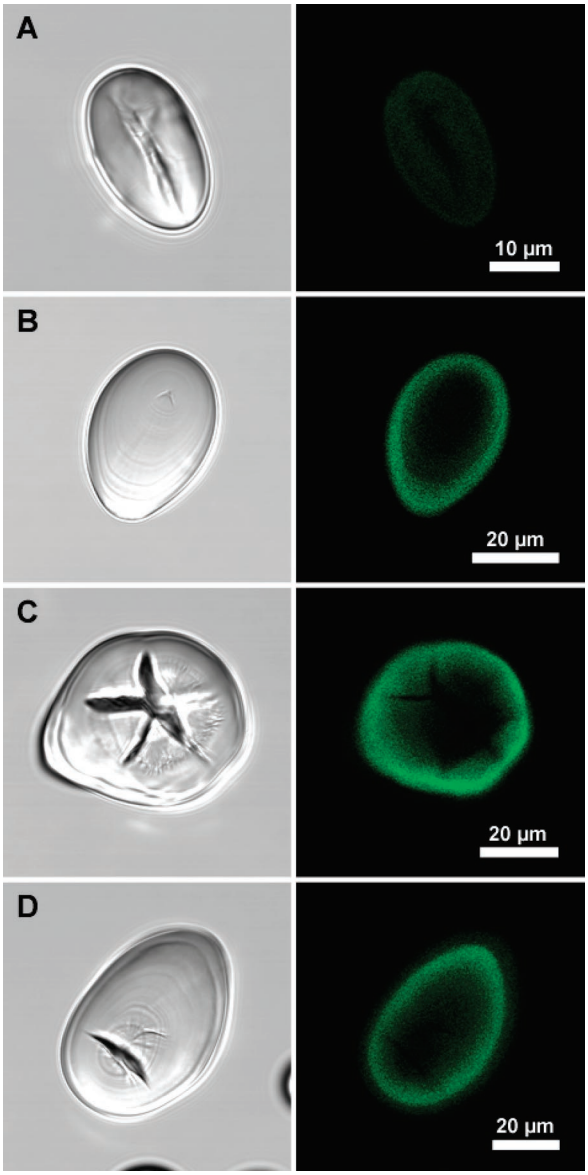

Figure 8. Pro-Q staining of wheat and potato granules. Transmission image (left panel) and Pro-Q fluorescence (right panel). (A) Side view of a wheat granule with the distinct equatorial groove. (B) Normal potato granule. (C) High amylose potato granule showing internal cracking. (D) High amylose potato granule showing more intense staining beneath the surface. Scale bars as indicated.

of APTS fluorescence leads to images with high resolution, and these are important properties when looking for details in surface images. We observed porelike structures on the surface of maize granules in the hundred nanometer range, showing that this technique is suitable for reasonably detailed surface studies. Taken together, the use of CLSM on APTS stained granules couples several already established methods of analyzing starch granules giving both internal and external structural information, as well as a detailed map of the starch molecule distribution in the granule.

APTS staining of carbohydrates was initially developed as a method for detection of gel-separated malto-oligosaccharides.[37,38] Blennow et al.[12] expanded further on the usefulness of APTS by reasoning that the equimolar labeling of starch molecules could be used to distinguish between amylose and amylopectin in native starch granules. Assuming a molecular weight of amylopectin of 100 times that of amylose in a granule with 20% amylose content, the ratio of amylose to amylopectin reducing ends is 25, clearly suggesting that amylose-rich regions should be more heavily labeled. Analysis of APTS labeled potato granules demonstrated the preferential labeling of amylose and showed that fluorescence intensity as imaged by CLSM was positively correlated to amylose content.[12] Staining with APTS will not only be influenced by the amylose and amylopectin distribution, but also by the specific distribution of reducing ends. If the large starch molecules participate in regular ordered structures, as has been shown for amylopectin, then this might be reflected in an uneven staining pattern. We observed growth rings in granules of *waxy* maize, a starch with no detectable amylose content, suggesting that this might indeed be the case. It is also reasonable to assume that the concentration of amylopectin reducing ends is high in the hilum where synthesis is initiated. The bright fluorescent dot seen in the hilum of some high amylopectin rice and *waxy* maize granules might reflect the labeling of amylopectin reducing ends. This fluorescent structure will not be visible in granules where the optical plane of sectioning has not passed through the hilum. How the reducing ends of amylopectin are distributed in the semicrystalline and amorphous layers of the granule is not known. Amylose has not been implicated in any regular ordered structures, though some level of cocrystallinity with amylopectin has been suggested.[39,40] Another source of staining unrelated to the starch molecules could be proteins and lipids present inside the starch granule, though the influence of these compounds on the observed staining pattern is not clear.

Observations of granule size and shape by both CLSM and SEM were in good accordance with published data.[23] The deposition of growth rings as viewed by APTS staining offers a potential explanation for the diverse shapes seen among the studied starch granules. It would appear that, depending on the botanical source, granules are shaped by either physical interactions with neighboring granules or the specific deposition of growth rings. Examples of the latter are the granules of pea and high amylose potato, both of which contain irregular growth rings that follow the outside surface. In pea, but not high amylose potato, the hilum appears as a diffuse, elongated structure around which the first growth rings are formed, offering a possible explanation for the irregular shape of these granules. In normal maize and tapioca granules, growth rings are deposited as regular round structures, and in the case of maize, these growth rings are often cut off at the surface, suggesting that growth-ring deposition has been discontinued or enhanced in certain areas of the granule surface. The most likely explanation for this observation is physical interaction with adjacent granules in the endosperm, which would prevent synthesis of new growth rings in areas of contact. Growth rings of tapioca were only observed around the hilum, but the shape of these granules also appears to be heavily influenced by interactions with neighboring granules. Starch granules from normal potato, barley, and wheat are laid down as regular rounded structures and do not appear to be come into contact with other granules during development. The only source of starch granules in which growth rings were not visible was rice. A simple explanation of this observation could be the small size of the granules. Alternatively, a more uniform distribution of amylose might obscure actual growth rings. Atomic force microscopy (AFM) images of sectioned rice granules have shown that the interior is made up of layers approximately 400 nm apart, though the orientation of these layers in relation to the granule surface was not clearly demonstrated.[41] Interestingly, the presence of triangular shapes of varying fluorescence intensity suggests that the mechanism of starch molecule deposition differs from maize starch, which shows a similar, yet less pronounced, polygonal granule shape with clear round growth rings. Using electron optical tomography and cryoelectron diffraction, Ostergetel and van Bruggen[2] concluded that the crystalline domains of amylopectin are built from continuous left-handed helical segments (superhelices) with a diameter of 18 nm. If the granule structure is built from straight segments of helical amylopectin deposited perpendicular to the growth rings, it is obvious that the curvature of the granule would interfere with the packing of rod-shaped superhelices. If the lack of visible growth rings in rice represents a deposition of crystalline amylopectin as flat layers, then any strain introduced by having to bend the crystalline arrays to form a circular structure would be eliminated. The presence of amorphous growth rings might be a mechanism designed to "reinitialize" the synthesis of the amylopectin superhelices, thus preventing excessive strain from having to fit the curved structure of the granule.

Surface images of wheat and barley did not reveal any of the equatorial grooves associated with these cereals. Internal CLSM images showed an uneven distribution of starch molecules along the equatorial groove, but despite this altered fluorescence pattern, growth rings were observed to go across the groove. The significance of this observation is not clear. It is possible that it represents an internal scar left after the development and expansion of the equatorial groove during granule development.

Channels were observed at varying frequencies in granules from wheat, barley, and maize. In wheat and maize, the channels were seen to transect the growth rings without any visible structural disturbance. Localized amylolytic activity taking place after completion of starch granule formation may have caused these channels. On the basis of identification of specific proteins in channels of maize, Fannon et al.[42] hypothesized that channels are formed when granules develop around radially oriented microtubules in the amyloplast. We also observed proteins in channels of maize, as did Han and Hamaker[26] in a previous CLSM study. On the basis of available data, no conclusions can be drawn concerning the origin of channels. It would be interesting to follow the formation of channels during starch granule development in the endosperm. Images of younger granules would determine whether channels are formed around microtubules or at a later stage of development.

Amylose concentration appears to be an important factor in determining starch granule integrity. We observed frequent internal cracks in granules from *waxy* maize and to a lesser

extent in granules from high amylose potato. Cracking in maize was primarily radial, suggesting less stability in the interactions between the radially arranged amylopectin molecules. In general, many larger granules showed internal cracking regardless of the botanical origin, suggesting an increasing strain on the amylopectin structure as the granule grows. Granules from high amylopectin rice displayed only minor internal cracking. If the strain on granule structure is at least partially dependent on size, then the small rice granules might never reach a size where internal strain on the amylopectin structure causes cracking. It cannot be ruled out that cracking is an artifact of granule preparation, but there appears to be a tendency of decreasing granule integrity in both high amylopectin and high amylose starches.

The high amylose starches from maize and potato showed irregular granule shapes containing multiple round fluorescent structures. In maize, these granules were often elongated, filamentous structures with the fluorescent bodies arranged like a string of pearls inside the elongated structures. A study of high amylose maize by Atkin et al.[11] showed that the round maize granules were normally birefringent, while the elongated structures were only weakly birefringent at the surface, indicating a lack of internal crystalline order. In contrast, polarization microscopy of potato granules indicated that the round fluorescent bodies represent the hila of individual radially built granules, consistent with the idea that aberrant initiation of new granules has led to the formation of these compound granule structures. It cannot be concluded exactly how these granule structures are formed, but given their smooth surface topography and the fact that the round granules of maize also show the multiple-hila structure, it is unlikely that they represent simple conglomerates of smaller granules. Very little is known about the mechanism of granule initiation. Mutations that reduce isoamylase activity in barley and potato lead to increased granule initiation.[43,44] It was suggested that isoamylase may function in suppressing the initiation of new glucan polymers from which new granules might arise.[43] In potato with reduced isoamylase activity, numerous smaller granules were often observed to form compound structures very similar to the structures observed in high amylose potato.[44] Many of the small granules were attached to the surface of larger granules, and the authors assumed that the compound structures were caused by clumping together of smaller granules.[44] Given the apparent lack of internal crystalline order in the elongated maize granules, it is possible that the amorphous content of these granules represents a structure reminiscent of the natural primer from which granules are formed, thus leading to multiple events of granule initiation by the responsible starch-synthesizing enzymes.

The high amylose maize starch belongs to the B-type crystalline polymorph as opposed to the A-type polymorph of normal and *waxy* maize.[35] It has been established that amylopectin chain length is a major contributor to the determination of crystalline polymorph,[5] and the longer average chain length of the high amylose maize starch may thus lead to a shift in crystalline polymorph. The shapes of the high amylose maize granules were rounded with smooth surfaces, a feature associated with the B-type polymorph potato granules. At the nanometer scale, the *waxy* maize granule surfaces were similar to granule surfaces from normal maize, except for the lower frequency of channel openings. The surface of high amylose potato was rough and pitted. In contrast to maize, high amylose potato contains high levels of phosphate esters, but the influence of phosphate on amylopectin structure is not known. Molecular modeling has suggested that phosphorylation at the C-3 position of the glucose units might interfere with double-helix packing.[15] The low phosphate potato starch has similar high amylose levels but very little starch-bound phosphate. Interestingly, the surfaces of these granules are smooth, implying that phosphate, rather than amylose, determines the surface characteristics of high amylose potato starch granules.

The presence of phosphate esters in amylopectin has profound effects on both the physicochemical properties of starch and its degradation in the plant.[15] Despite this, little is known about the effects of phosphate on starch structure and digestability. Mutations in the major starch phosphorylating enzyme lead to starch-excess phenotypes due to impaired starch degradation.[45,46] It has been suggested that the activity of amylolytic enzymes might rely on direct interaction with phosphate groups or that the inclusion of phosphate affects the physicochemical properties of amylopectin, thereby facilitating enzymatic attack.[15,47] We have demonstrated that the fluorescent probe Pro-Q Diamond functions as a probe for phosphate in native starch granules. The fluorescence intensity of stained potato granules was positively correlated to the content of starch-bound phosphate. In contrast to cereal starches, phosphate esters are the only significant source of phosphate in potato granules.[17] The intense staining associated with the surface could reflect an increased concentration of accessible phosphate near the granule surface. Although these results seem to conflict with the previous observation that phosphate is more concentrated near the granule core,[13,18] the surface staining pattern may reflect a more physiologically relevant fraction of phosphate monoesters, since evidence from potato indicates that degradation of transient starch in leaves is accompanied by an initial increase in phosphorylation of the starch granule surface.[48] If phosphorylation during degradation represents a direct signal for subsequent attack by amylolytic enzymes, it follows that surface-bound phosphate groups must be accessible for these interactions to occur. This would imply a model of starch surface structure that differs from the generally accepted models of amylopectin structure. Whether the increase in surface phosphorylation during degradation is a consequence of an altered surface structure or vice versa is not known. Staining of broken potato granules demonstrated that Pro-Q had less affinity for exposed internal structures, suggesting either lower concentrations of phosphate in the interior or that phosphate groups at the surface are more accessible to the dye. This can also be concluded from the analyses of high amylose potato granules, where internal cavities were left unstained and fluorescence was concentrated just beneath the surface. These results strongly suggest that Pro-Q interactions are specific and phosphate-dependent. Furthermore, if binding of Pro-Q is unspecific and limited to granule surfaces, then staining of channels and cavities in maize and wheat is also to be expected. This has previously been observed by reaction with phosphoryl chloride[42] and staining with merbromin.[25] The uniform staining of *Curcuma zedoaria* granules suggests a phosphate distribution different from potato, but one must bear in mind that these granules are disc-shaped and much thinner, meaning that the CLSM optical section is less likely to pass through the granule core. We have observed significant surface staining in some granules of *Curcuma zedoaria* when viewed from the side (data not shown).

Although the cereal starches were considerably less fluorescent than the potato starches after Pro-Q staining, they were nevertheless more intensely stained than expected, given their minimal content of starch-bound phosphate. Cereal starches contain phosphate primarily in the form of phospholipids, in amounts positively correlated to the amylose content.[20] An

analysis of *waxy* maize, which contains only trace amounts of total phosphate, showed an almost complete absence of staining in most granules, suggesting that the source of staining observed in normal maize could be phospholipids present in the granule. It is possible that Pro-Q could act as a probe for phospholipids in cereal starches where the content of starch-bound phosphate is minimal. In that case, these results indicate that phospholipids are evenly distributed across the granule.

Acknowledgment. We thank Per Lassen Nielsen for technical assistance and Michael Hansen for assistance with confocal laser scanning microscopy. This project was supported by the Committee for Research and Development of the Øresund Region (Øforsk), the Danish National Research Foundation, and a grant from the Danish Research Council for Technology and Production Sciences (grant no. 23-04-0239).

References and Notes

(1) Buléon, A.; Colonna, P.; Planchot, V.; Ball, S. *Int. J. Biol. Macromol.* **1998**, *23*, 85−112.
(2) Oostergetel, G. T.; van Bruggen, E. F. J. *Carbohydr. Polym.* **1993**, *21*, 7−12.
(3) Gallant, D. J.; Bouchet, B.; Baldwin, P. M. *Carbohydr. Polym.* **1997**, *32*, 177−191.
(4) Imberty, A.; Buléon, A.; Tran, V.; Pérez, S. *Starch/Stärke* **1991**, *43*, 375−384.
(5) Hizukuri, S. *Carbohydr. Res.* **1985**, *141*, 295−306.
(6) Tatge, H.; Marchall, J.; Martin, C.; Edwards, A.; Smith, A. M. *Plant Cell Environ.* **1999**, *22*, 543−550.
(7) Cooke, D.; Gidley, M. J. *Carbohydr. Res.* **1992**, *227*, 103−112.
(8) Bogracheva, T. Y.; Cairns, P.; Noel, T. R.; Hulleman, S.; Wang, T. L.; Morris, V. J.; Ring, S. G.; Hedley, C. L. *Carbohydr. Polym.* **1999**, *39*, 303−314.
(9) Jane, J.; Xu, A.; Radosavljevic, M.; Seib, P. A. *Cereal Chem.* **1992**, *69*, 405−409.
(10) Kuipers, A. G. J.; Jacobsen, E.; Visser, R. G. F. *Plant Cell* **1994**, *6*, 43−52.
(11) Atkin, N. J.; Cheng, S. L.; Abeysekera, R. M.; Robards, A. W. *Starch/Stärke* **1999**, *51*, 163−172.
(12) Blennow, A.; Hansen, M.; Schulz, A.; Jørgensen, K.; Donald, A. M.; Sanderson, J. *J. Struct. Biol.* **2003**, *143*, 229−241.
(13) Jane, J. L.; Shen, J. J. *Carbohydr. Res.* **1993**, *247*, 279−290.
(14) Nielsen, T. H.; Wischmann, B.; Enevoldsen, K.; Møller, B. L. *Plant Physiol.* **1994**, *105*, 111−117.
(15) Blennow, A.; Engelsen, S. B.; Nielsen, T. H.; Baunsgaard, L.; Mikkelsen, R. *Trends Plant Sci.* **2002**, *7*, 445−450.
(16) Kasemsuwan, T.; Jane, J. L. *Cereal Chem.* **1996**, *73*, 702−707.
(17) Lim, S. T.; Kasemsuwan, T.; Jane, J. L. *Cereal Chem.* **1994**, *71*, 488−493.
(18) Blennow, A.; Sjöland, A. K.; Anderson, R.; Kristiansson, P. *Anal. Biochem.* **2005**, *347*, 327−329.
(19) Blennow, A.; Bay-Smidt, A. M.; Olsen, C. E.; Møller, B. L. *Int. J. Biol. Macromol.* **2000**, *27*, 211−218.
(20) Morrison, W. R.; Law, R. V.; Snape, C. E. *J. Cereal Sci.* **1993**, *18*, 107−109.
(21) Mu-Forster, C.; Huang, R.; Powers, J. R.; Harriman, R. W.; Knight, M.; Singletary, G. W.; Keeling, P. L.; Wasserman, B. P. *Plant Physiol.* **1996**, *111*, 821−829.
(22) Borén, M.; Larsson, H.; Falk, A.; Jansson, C. *Plant Sci.* **2004**, *166*, 617−626.
(23) Jane, J. L.; Kasemsuwan, T.; Leas, S.; Zobel, H.; Robyt, J. *Starch/Stärke* **1994**, *46*, 121−129.
(24) van de Velde, F.; van Riel, J.; Tromp, R. H. *J. Sci. Food Agric.* **2002**, *82*, 1528−1536.
(25) Huber, K. C.; BeMiller, J. N. *Carbohydr. Polym.* **2000**, *41*, 269−276.
(26) Han, X.-Z.; Hamaker, B. R. *J. Cereal Sci.* **2002**, *35*, 109−116.
(27) Huber, K. C.; BeMiller, J. N. *Cereal Chem.* **1997**, *74*, 537−541.
(28) Planchot, V.; Roger, P.; Colonna, P. *Starch/Stärke* **2000**, *52*, 333−339.
(29) Viksø-Nielsen, A.; Blennow, A.; Jørgensen, K.; Kristensen, K. H.; Jensen, A.; Møller, B. L. *Biomacromolecules* **2001**, *2*, 836−843.
(30) Bay-Smidt, A. M.; Wischmann, B.; Olsen, C. E.; Nielsen, T. H. *Starch/Stärke* **1994**, *46*, 167−172.
(31) Blennow, A.; Bay-Smidt, A. M.; Wischmann, B.; Olsen, C. E.; Møller, B. L. *Carbohydr. Res.* **1998a**, *307*, 45−54.
(32) Blennow, A.; Bay-Smidt, A. M.; Olsen, C. E.; Møller, B. L. *J. Chromatogr., A* **1998b**, *829*, 385−391.
(33) Hovenkamp-Hermelink, J. H. M.; De Vries, J. N.; Adamse, P.; Jacobsen, E.; Witholt, B.; Feenstra, W. J. *Potato Res.* **1988**, *31*, 241−246.
(34) Oates, C. G. *Trends Food Sci. Technol.* **1997**, *8*, 375−382.
(35) Shi, Y. C.; Capitani, T.; Trzasko, P.; Jeffcoat, R. *J. Cereal Sci.* **1998**, *27*, 289−299.
(36) Engelsen, S. B.; Madsen, A. Ø.; Blennow, A.; Motawia, M. S.; Møller, B. L.; Larsen, S. *FEBS Lett.* **2003**, *541*, 137−144.
(37) O'Shea, M. G.; Morell, M. K. *Electrophoresis* **1996**, *17*, 681−688.
(38) O'Shea, M. G.; Samuel, M. S.; Konik, C. M.; Morell, M. K. *Carbohydr. Res.* **1998**, *307*, 1−12.
(39) Blanshard, J. M. V. In *Critical reports on applied chemistry volume 13, Starch: Properties and Potential*; Galliard, T., Ed.; John Wiley & Sons: Chichester, 1987; pp 16−54.
(40) Jenkins, P. J.; Donald, A. M. *Int. J. Biol. Macromol.* **1995**, *17*, 315−321.
(41) Dang, J. M. C.; Copeland, L. *J. Cereal Sci.* **2003**, *37*, 165−170.
(42) Fannon, J. E.; Gray, J. A.; Gunawan, N.; Huber, K. C.; BeMiller, J. N. *Cellulose* **2004**, *11*, 247−254.
(43) Burton, R. A.; Jenner, H.; Carrangis, L.; Fahy, B.; Fincher, G. B.; Hylton, C.; Laurie, D. A.; Parker, M.; Waite, D.; van Wegen, S.; Verhoeven, T.; Denyer, K. *Plant J.* **2002**, *31*, 97−112.
(44) Bustos, R.; Fahy, B.; Hylton, C. M.; Seale, R.; Nebane, N. M.; Edwards, A.; Martin, C.; Smith, A. *Proc. Natl. Acad. Sci. U.S.A.* **2004**, *101*, 2215−2220.
(45) Lorberth, R.; Ritte, G.; Willmitzer, L.; Kossman, J. *Nat. Biotechnol.* **1998**, *16*, 473−477.
(46) Yu, T.-S.; Kofler, H.; Häusler, R. E.; Hille, D.; Flügge, U.-I.; Zeeman, S. C.; Smith, A. M.; Kossman, J.; Lloyd, J.; Ritte, G.; Steup, M.; Lue, W.-L.; Chen, J.; Weber, A. *Plant Cell* **2001**, *13*, 1907−1918.
(47) Ritte, G.; Lloyd, J. R.; Eckermann, N.; Rottmann, A.; Kossman, J.; Steup, M. *Proc. Natl. Acad. Sci. U.S.A.* **2002**, *99*, 7166−7171.
(48) Ritte, G.; Scharf, A.; Eckermann, N.; Haebel, S.; Steup, M. *Plant Phys.* **2004**, *135*, 1−10.

BM060216E